

KALMAN FILTER APPLIED TO ULTRASSONIC-BASED LEVEL SENSING

André Avelãs Machado de Araujo, andremdaraujo@usp.br

Rafael Lino de Lima, rafael.lino@usp.br

Pedro Cardozo de Mello, pcmello@usp.br

Mario Luis Carneiro, micarneiro@usp.br

Eduardo Aoun Tannuri, eduat@usp.br

Escola Politécnica, University of São Paulo – Department of Mechatronics Engineering
Numerical Offshore Tank Laboratory (TPN-USP)
Av. Prof. Mello Moraes, 2231 – Cidade Universitária, 05508-030 – São Paulo – SP – Brasil

Abstract. *The following project suggests the use of a Kalman Filter for conditioning wave height signals, acquired from ultrasonic sensors present in the new wave basin of TPN ("Tanque de Provas Numérico", Portuguese for "Numeric Offshore Tank"), recently constructed in University of São Paulo – USP, named Hydrodynamic Calibrator (CH-TPN). The sensors are mounted on the frontal face of each of the 148 flaps present in the tank, and are responsible for the incident wave height measurements. These measurements are directly used in the active wave absorption algorithm, which is the great advantage of the tank. Currently, the wave height signals present noise and distortion, mainly due to mechanical problems that occurred during the sensors installation, which lead to spurious ultrasonic echoes and inaccurate wave height measurements. A low pass filter is being used to attenuate the signal noise together with a sensor mapping which exclude the worse sensors, but this configuration has three main disadvantages in this application: it delays the signal, which compromises severely the absorption control; presents a significant loss in wave height signal when the noise is more intense; and worsens multi-directional waves absorption. Aiming to have a better signal on each flap, it is suggested the use of the Kalman Filter, which is an "intelligent" filter, since it takes into count the system dynamic model and estimates the measurements weighting between the predictions and the values acquired by the sensors themselves. Another interesting feature of this kind of filter is that it allows sensor fusion, that is, it allows the use of more than one sensor to evaluate the same measurement, thus improving the estimation. The project involved designing the Kalman Filter to work with two different kinds of waves: regular waves, which have a constant and unique frequency; and irregular waves, which have a wide frequency spectrum. With the use of the Kalman Filter, it was expected that the wave re-reflection coefficient would be reduced from about 15% to about 5%, which is the value originally expected in the wave basin design. The project was divided in five basic phases: theoretical study, offline implementation, online implementation, tests and data acquisition, and finally, documentation of results. After implementation and tests, it was confirmed that the use of Kalman Filter applied to the wave height sensors enabled great improvement in both signal quality and absorption. However, it was not possible to utilize the Filter simultaneously in all 148 sensors due to little time available to perform its calculations. Still, it was possible to run the absorption algorithm and the Kalman filter for a full wall of the tank (39 flaps simultaneously). Several trials were held to evaluate objectively the performance improvement using the Filter. The expected reduction in the re-reflection coefficient, of about 5% to 10%, was achieved in most of the trials, proving the Filter's efficiency and thus providing a new component in the CH-TPN software library.*

Keywords: *Kalman, Filter, Wave, Basin, Absorption*

1. INTRODUCTION

Conceived with the purpose of calibrating hydrodynamic and structural models used in TPN® simulator, the CH-TPN (Hydrodynamic Calibrator of TPN) was designed to reduce time and complexity of the trials. Showing great versatility and flexibility due to the high degree of automation, the new facility allows execution of ocean systems trials in regular or random waves, minimizing the influences of reflected waves through an innovative system of flaps that generate and absorb the waves. The speed and simplicity of obtaining hydrodynamic coefficients, the ability to quickly test conceptual models of floating units and the basic investigation of nonlinear and second order phenomena are among the advantages offered by the hydrodynamic calibrator (TPN, 2010).

The Hydrodynamic Calibrator is a squared basin with sides measuring 14 meters. The water depth is 4 meters. Each of its four walls has movable flaps (two walls with 39 and the other two with 35 flaps), summing a total of 148. Next, Fig. 1 shows the CH-TPN facility. For more detail about the wave basin, refer to Carneiro *et. al.* (2009).



Figure 1. Hydrodynamic Calibrator of TPN – CH-TPN (TPN, 2010)

In CH-TPN, the wave height values on each flap are crucial parameters since they are directly used in the active wave absorption algorithm. Currently, the wave height signals obtained from ultrasonic sensors that are mounted on the frontal face of each flap, present noise and distortion. This is caused mainly due to mechanical problems that occurred during the sensors installation, leading to spurious ultrasonic echoes and inaccurate wave height measurements. This condition of the signal does not allow the basin to work on its full wave absorption capacity, thus, results in less precise simulations in TPN.

Aiming to have a better signal on each flap, it is suggested the use of the Kalman Filter, which is an “intelligent” filter, since it takes into account the system dynamic model and estimates the measurements weighting between the predictions and the values acquired by the sensors themselves. Another interesting feature of this kind of filter is that it allows the so called sensor fusion, that is, it allows the use of more than one sensor to evaluate the same measurement, therefore improving the estimation.

Currently, a second order Butterworth low pass filter is being used to attenuate the signal noise, but this kind of filter has two main disadvantages in this application. Firstly it delays the signal, which compromises severely the absorption control and secondly it presents a significant loss in wave height signal when the noise is more intense. Also, sensors are linked to flaps using a mapping that exclude the worse sensors. Therefore, a sensor could be driving two or even three adjacent flaps. This configuration greatly improved the absorption rates in the wave basin for frontal waves, i.e., waves that strike the absorbing flaps perpendicularly. However, waves with different directions are poorly absorbed since flaps working with the same sensor reduce wall’s discretization. With the use of Kalman Filter, it is expected that the sensor mapping may be removed and the directional waves’ absorption could be improved.

2. METODOLOGY

This project (Araujo *et al.*, 2010) was divided in five main steps:

- Theoretical study
- Offline implementation
- Online implementation
- Tests and data acquisition
- Documentation of results

The theoretical study phase comprises of both the Kalman Filter mathematical formulation and the real problem modeling.

The implementation was separated into two steps. The first, offline, served as an evaluation of the feasibility to apply the Filter to the real problem. In this part, previously acquired signals from tests held in the basin served as input to the Filter algorithm.

Once verified the Filter behavior and the actual improvement in the wave height signal, then it was possible to start the second step, which is basically adapt the offline Filter software in a way that it can be used online, real time, integrated in the basin’s control system (based on Simulink tool of MATLAB®).

After solving all issues regarding the online implementation, it was time to move to the performance tests of the Filter and data acquisition for later analysis as a means to have an objective evaluation of the Kalman Filter effectiveness in this application.

3. IMPLEMENTATION

3.1. Kalman Filter formulation

The Kalman Filter (Kalman, 1960; Grewal, Andrews, 2008) estimates a process state, at a given time, by comparison between a mathematical model and the measurements acquired by the sensors, weighting according to the model and measurement inaccuracies (\mathbf{Q} and \mathbf{R} Kalman parameters), resulting in an optimum estimate.

A system modeled in state-space can be represented as shown in Eq. 1 and Eq. 2, below:

$$\mathbf{x}_k = \mathbf{A} \cdot \mathbf{x}_{k-1} + \mathbf{B} \cdot \mathbf{u}_k + \mathbf{w}_{k-1} \quad (1)$$

$$\mathbf{z}_k = \mathbf{H} \cdot \mathbf{x}_k + \mathbf{v}_k \quad (2)$$

where:

- \mathbf{x}_k is the state vector in time step k ;
- \mathbf{A} is the state matrix;
- \mathbf{B} is the input matrix;
- \mathbf{u}_k is the input vector in time step k ,
- \mathbf{w}_{k-1} is the process noise;
- \mathbf{z}_k is the measurement of the state \mathbf{x}_k in time step k ;
- \mathbf{H} is the matrix which relates the actual state with the measurement; and
- \mathbf{v}_k is the measurement noise.

First, the Filter predicts the current state of the system using only information obtained in the last time step estimate (or initial parameters, if it is the first iteration), as seen in Eq. 3 (*a priori* estimate, $\hat{\mathbf{x}}_k^-$).

$$\hat{\mathbf{x}}_k^- = \mathbf{A} \cdot \hat{\mathbf{x}}_{k-1} + \mathbf{B} \cdot \mathbf{u}_k \quad (3)$$

Then, in Eq. 4, using the process noise covariance, \mathbf{Q} , it is calculated the prediction covariance, \mathbf{P}_k^- .

$$\mathbf{P}_k^- = \mathbf{A} \cdot \mathbf{P}_{k-1} \cdot \mathbf{A}^T + \mathbf{Q} \quad (4)$$

The prediction covariance, \mathbf{P}_k^- , together with the measurement noise covariance, \mathbf{R} , are used in Eq. 5 to calculate the Kalman gain, \mathbf{K}_k .

$$\mathbf{K}_k = \mathbf{P}_k^- \cdot \mathbf{H}^T \cdot (\mathbf{H} \cdot \mathbf{P}_k^- \cdot \mathbf{H}^T + \mathbf{R})^{-1} \quad (5)$$

Finally, in Eq. 6, the optimal estimate (*a posteriori* estimate, $\hat{\mathbf{x}}_k$) is obtained as a weighted mean between the first estimate (*a priori*) and the measurement \mathbf{z}_k .

$$\hat{\mathbf{x}}_k = \hat{\mathbf{x}}_k^- + \mathbf{K}_k \cdot (\mathbf{z}_k - \mathbf{H} \cdot \hat{\mathbf{x}}_k^-) \quad (6)$$

Before starting the next iteration, it is necessary to update the prediction covariance, \mathbf{P}_k , using Eq. 7.

$$\mathbf{P}_k = (\mathbf{I} - \mathbf{K}_k \cdot \mathbf{H}) \cdot \mathbf{P}_k^- \quad (7)$$

3.2. Real problem modeling

To apply the Filter to CH-TPN, the system to be modeled is the water; more specifically, the movement of water's surface – the wave height. As there are two different types of waves generated in the wave basin, two approaches are needed.

3.2.1. Regular waves

For regular waves, which have a constant and unique frequency, the wave height can be modeled as a sine wave with variable amplitude, as described in Eq. 8:

$$\mathbf{x}(t) = \mathbf{a}(t) \cdot \sin(\omega t) \quad (8)$$

where:

- \mathbf{x} is the wave height in instant t ;
- $\mathbf{a}(t)$ is the wave amplitude in instant t ;
- ω is the wave angular frequency.

Assuming the hypothesis that the variation in wave amplitude is a lot slower than the variation of the sine function, with respect to time, it is possible to derive the following differential equation of water movement (Eq. 9):

$$\ddot{\mathbf{x}} = -\omega^2 \mathbf{x} \quad (9)$$

where $\ddot{\mathbf{x}}$ is the second derivative of $\mathbf{x}(t)$ with respect to time. Going from continuous to discrete time, comes Eq. 10:

$$\begin{aligned} \frac{x_k - 2x_{k-1} + x_{k-2}}{\Delta t^2} &= -\omega^2 x_k \\ \Rightarrow (1 + \omega^2 \Delta t^2) x_k &= 2x_{k-1} - x_{k-2} \\ \therefore x_k &= \frac{1}{1 + \omega^2 \Delta t^2} (2x_{k-1} - x_{k-2}) \end{aligned} \quad (10)$$

where Δt is the time step of discretization.

Now, rewriting the equation in the matrix form yields the state space representation of the system (Eq. 11):

$$\begin{pmatrix} x_k \\ x_{k-1} \end{pmatrix} = \begin{bmatrix} \frac{2}{1 + \omega^2 \Delta t^2} & \frac{-1}{1 + \omega^2 \Delta t^2} \\ 1 & 0 \end{bmatrix} \begin{pmatrix} x_{k-1} \\ x_{k-2} \end{pmatrix} + \begin{pmatrix} w_1 \\ w_2 \end{pmatrix} \quad (11)$$

where w_i is the process noise, which includes modeling approximations.

Thus, the Kalman Filter A and B matrixes are (Eq. 12 and Eq. 13):

$$\mathbf{A} = \begin{bmatrix} \frac{2}{1 + \omega^2 \Delta t^2} & \frac{-1}{1 + \omega^2 \Delta t^2} \\ 1 & 0 \end{bmatrix} \quad (12)$$

$$\mathbf{B} = \mathbf{0} \quad (13)$$

In this case, the sensors have no dynamics, therefore the measurement z_k equals the wave height x_k in time step k , as show in Eq. 14.

$$z_k = (1 \ 0) \begin{pmatrix} x_k \\ x_{k-1} \end{pmatrix} + v_k \quad (14)$$

where v_k is the process noise, which includes modeling approximations.

Hence, the Kalman Filter H matrix is (Eq. 15):

$$\mathbf{H} = (1 \ 0) \quad (15)$$

3.2.2. Irregular waves

In the case of irregular waves, which have a wide frequency spectrum, the system approximation is made in the frequency domain, differently to the case of regular waves which are approximated in time domain. To do so, a second order transfer function developed by Pierson and Moskowitz in 1963 (Fossen, 1994; Eq. 16) is used to approximate the spectrum.

$$h(s) = \frac{2 \zeta \omega_0 \sigma_w s}{s^2 + 2 \zeta \omega_0 s + \omega_0^2} \quad (16)$$

where:

- ζ is the damping coefficient;
- ω_0 is nominal angular frequency;

- σ_w is a constant proportional to the intensity of the wave.

Similarly to what was done in the case of regular waves, a differential equation of the wave height movement (Eq. 17) can be derived from the Eq. 16 and, after discretizing it, the state space system is obtained (Eq. 18):

$$\ddot{y}(t) + 2 \zeta \omega_0 \dot{y}(t) + \omega_0^2 y(t) = K_w \dot{w}(t) \tag{17}$$

$$\begin{pmatrix} y_k \\ y_{k-1} \end{pmatrix} = \begin{bmatrix} \frac{2+2 \zeta \omega_0 \Delta t}{1+\omega_0^2 \Delta t^2+2 \zeta \omega_0 \Delta t} & \frac{-1}{1+\omega_0^2 \Delta t^2+2 \zeta \omega_0 \Delta t} \\ 1 & 0 \end{bmatrix} \begin{pmatrix} y_{k-1} \\ y_{k-2} \end{pmatrix} + \begin{pmatrix} w_1 \\ w_2 \end{pmatrix} \tag{18}$$

As a result, the Kalman Filter A and B matrixes are (Eq. 19 and Eq. 20):

$$A = \begin{bmatrix} \frac{2+2 \zeta \omega_0 \Delta t}{1+\omega_0^2 \Delta t^2+2 \zeta \omega_0 \Delta t} & \frac{-1}{1+\omega_0^2 \Delta t^2+2 \zeta \omega_0 \Delta t} \\ 1 & 0 \end{bmatrix} \tag{19}$$

$$B = 0 \tag{20}$$

The relation between the measurement and the actual wave height is still the same as Eq. 14, (Eq. 21):

$$z_k = (1 \ 0) \begin{pmatrix} y_k \\ y_{k-1} \end{pmatrix} + v_k \tag{21}$$

And so, the Kalman Filter H matrix is (Eq. 22):

$$H = (1 \ 0) \tag{22}$$

3.3. Offline implementation preliminary results

Below, Fig. 2 shows a wave height signal obtained in CH-TPN. Noticeably, the signal contains a significant noise component. The noise results in abrupt movements of the absorbing flaps, not only worsening the absorption performance but also generating spurious waves that destabilize the absorption control.

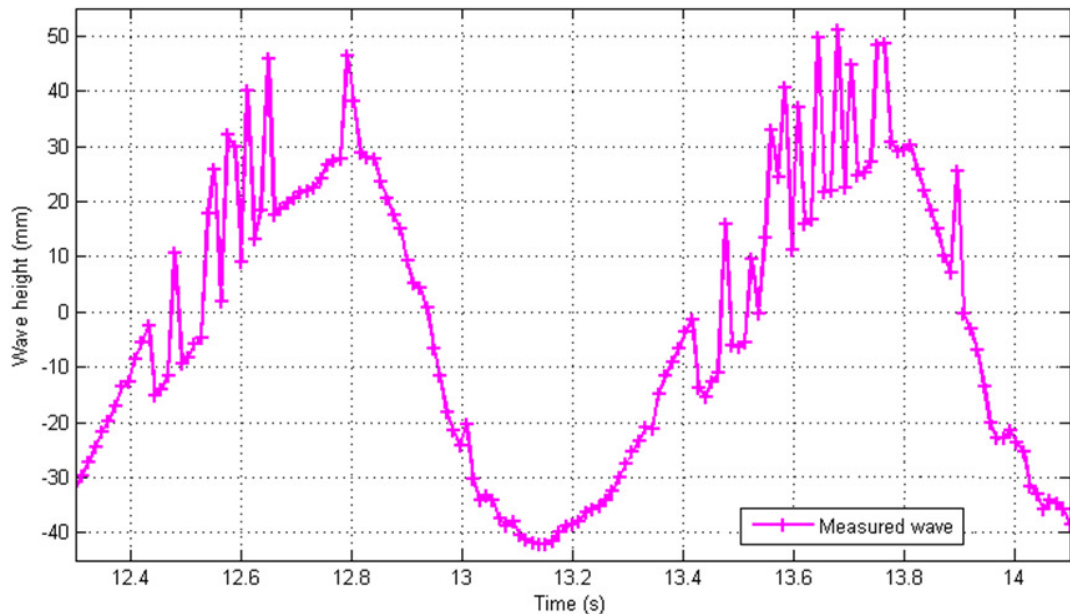


Figure 2. Wave height signal originally acquired by an ultrasonic sensor

In Fig. 3, after the Kalman filtering, it is possible to notice that great part of the signal was recovered in addition to great noise attenuation. This result was obtained in the offline processing. It is important to compare the Kalman filter against the low pass filter that was being used in CH-TPN (a second order Butterworth low pass filter, with cutoff

frequency of 8 Hz). With the low pass filter, there is a significant wave height loss when the signal rises, as well as a delay of approximately 3 time steps, in comparison to the original signal.

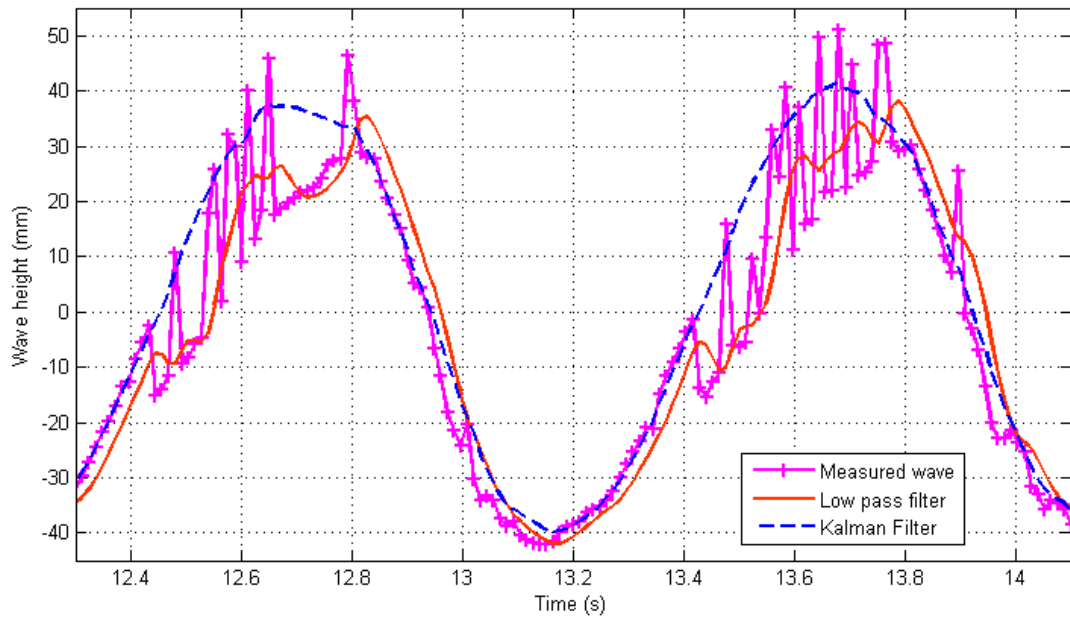


Figure 3. Comparison between measured wave height, low pass filter signal and Kalman Filter signal

The same Kalman Filter algorithm can be applied to irregular waves. The only need is to modify the system dynamic model. This system, a second order transfer function developed by Pierson and Moskowitz in 1963 (Fossen, 1994, Eq. 16), has parameters that are obtained empirically by fitting its frequency response over the desired wave spectrum, as seen in Fig. 4, below.

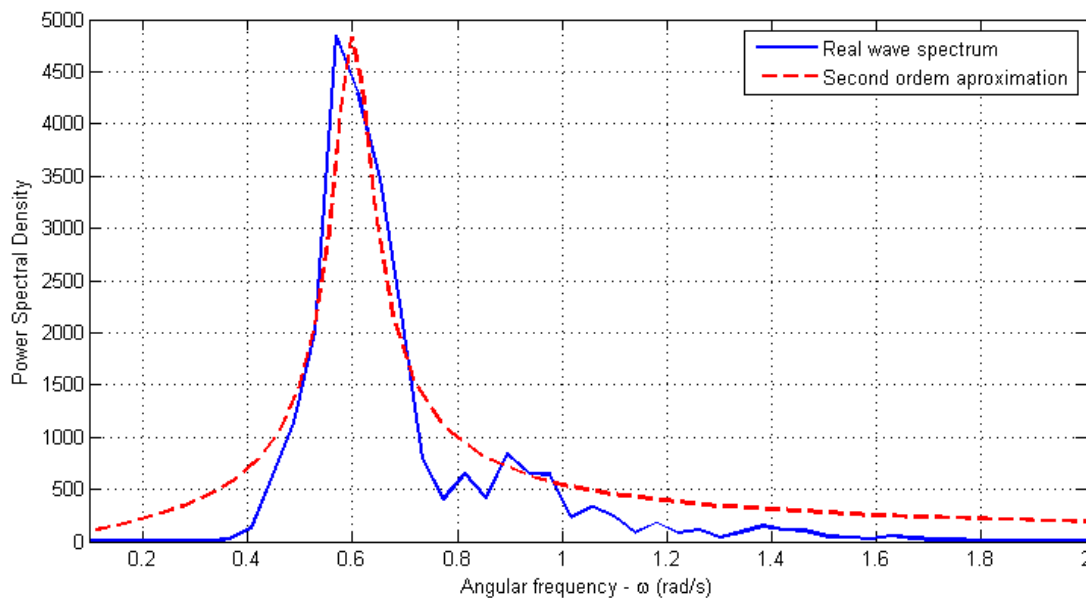


Figure 4. Irregular wave spectrum and second order system frequency response

Figure 5 shows a comparison between the original wave height signal and the offline Kalman filtered signal, confirming the result achievable using this Filter.

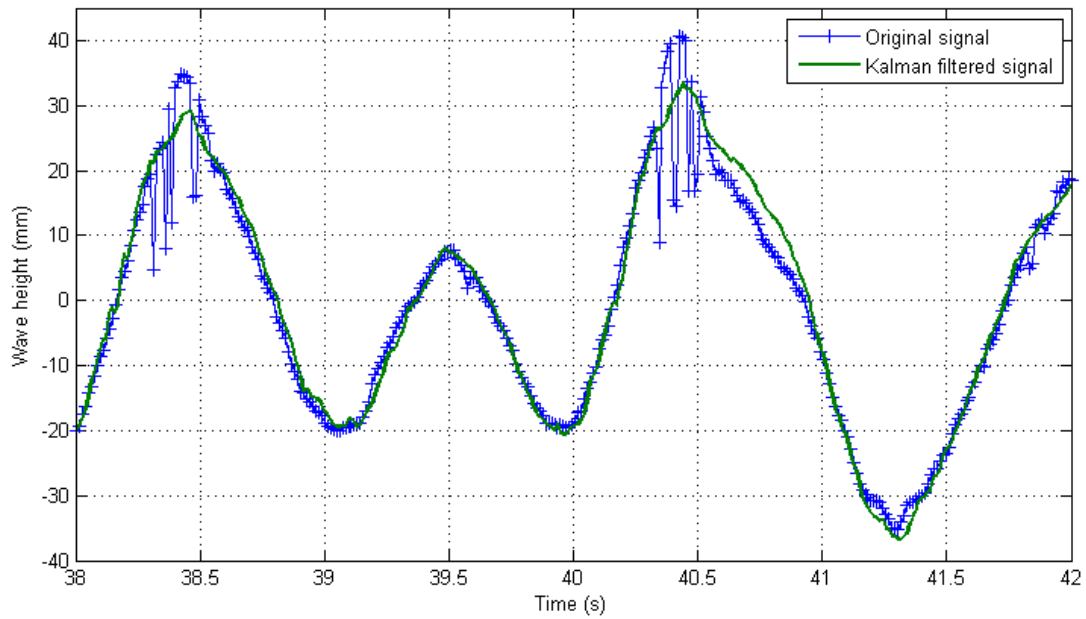


Figure 5. Detail of comparison between measured wave height and Kalman filtered signal

Similarly to what was verified before in the case of regular waves, it is possible to improve the measurement results, reducing noise and delay when compared to the low pass filter.

4. RESULTS

This chapter shows the results obtained during the online implementation of the Kalman Filter. More detail about the implementation and results can be found in Araujo *et al.* (2010) and Mello *et al.* (2010).

First, a qualitative analysis was done. The subsequent 4 figures (Fig. 6 to Fig. 9) show how effective the Kalman Filter was for regular waves (trials were done generating waves with four frequencies: 0.75, 1.00, 1.25 and 1.50 Hz, one at a time). All these plots were taken from the same sensor, so it is possible to visualize the effect of increasing frequency both in the original and in the filtered signals.

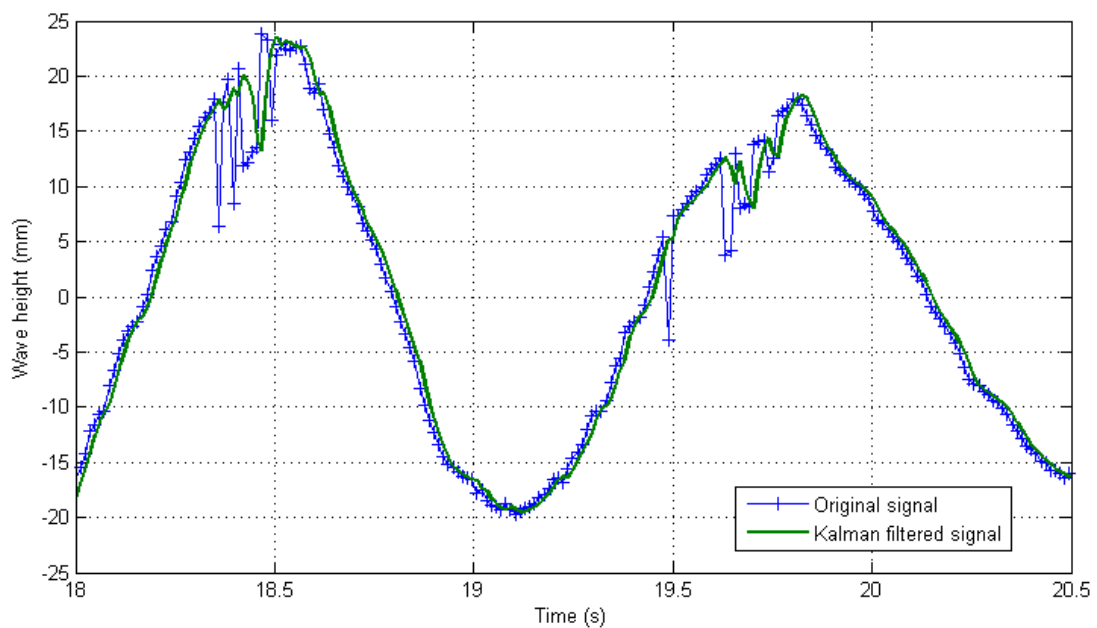


Figure 6. Comparison between wave height signals before and after Kalman filtering (wave frequency: 0.75 Hz)

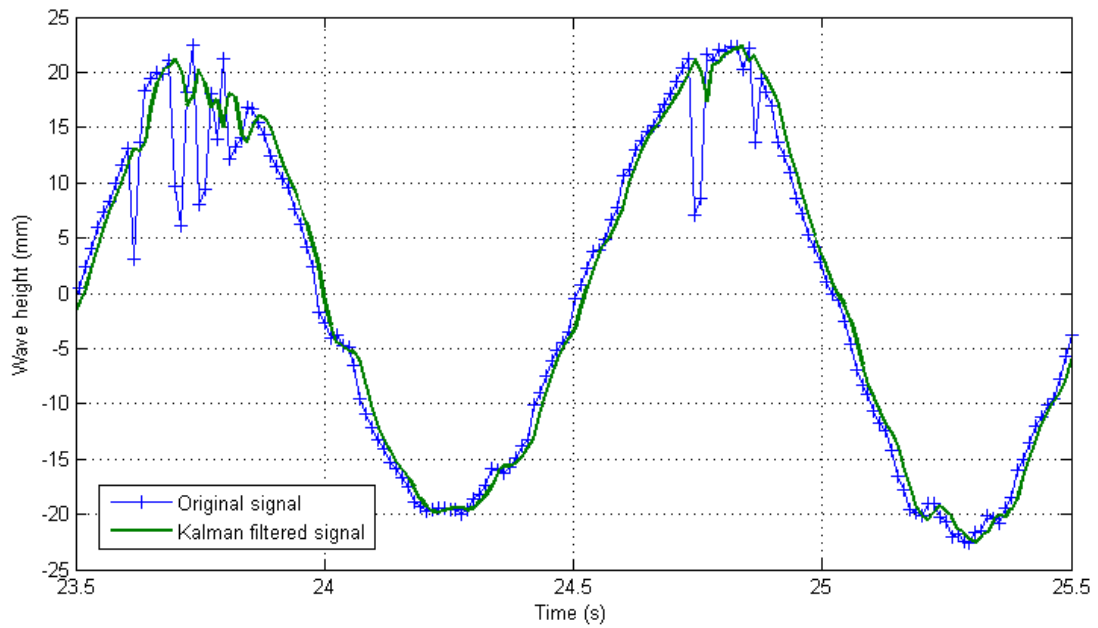


Figure 7. Comparison between wave height signals before and after Kalman filtering (wave frequency: 1.00 Hz)

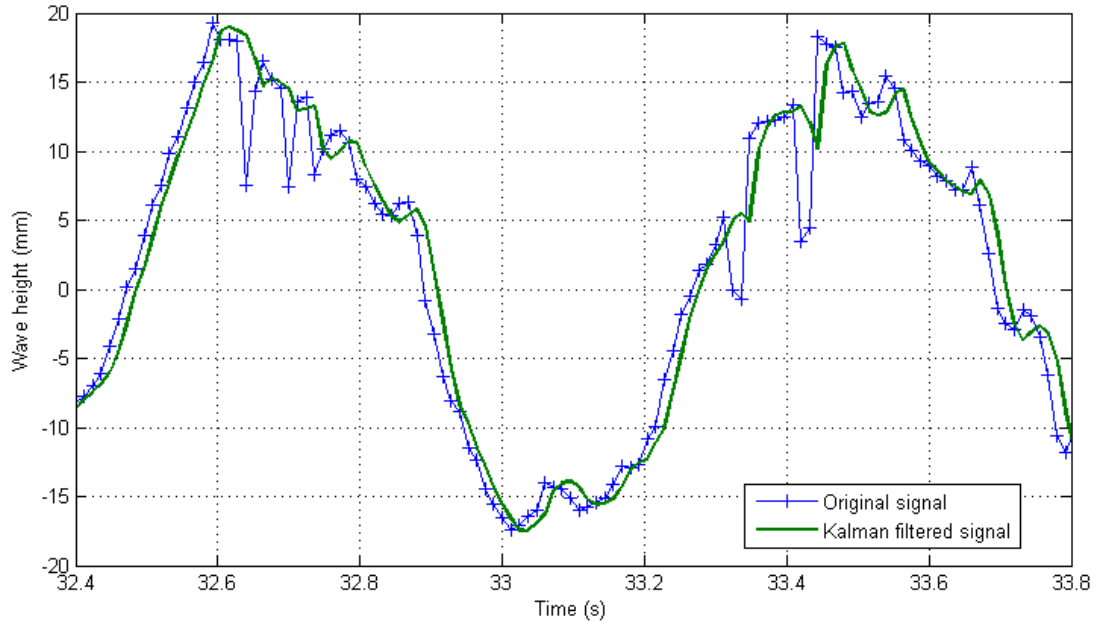


Figure 8. Comparison between wave height signals before and after Kalman filtering (wave frequency: 1.25 Hz)

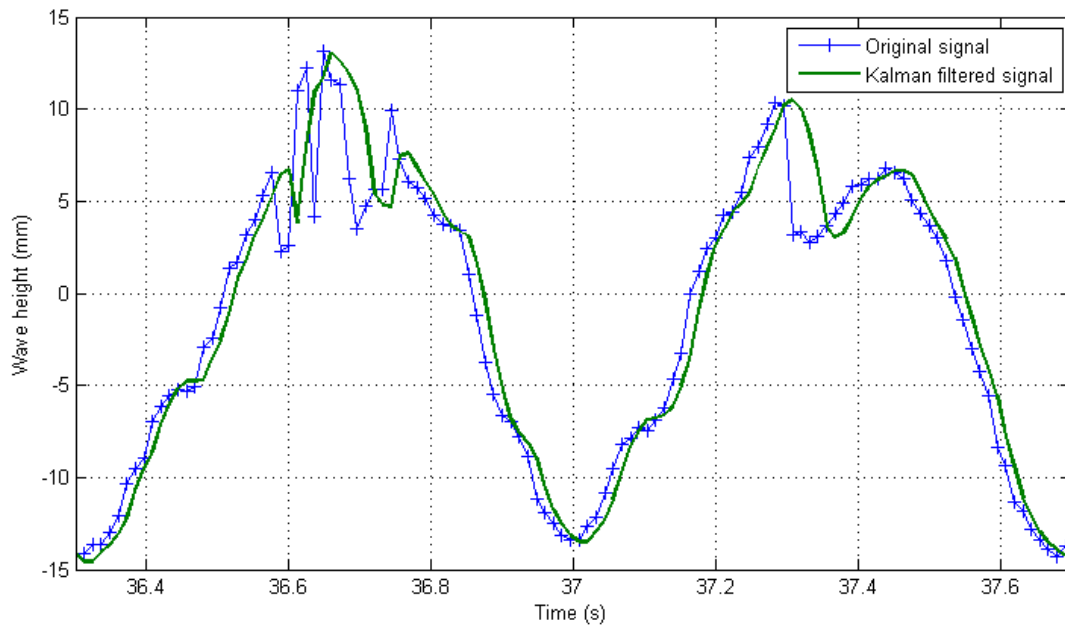


Figure 9. Comparison between wave height signals before and after Kalman filtering (wave frequency: 1.50 Hz)

The results show that the Filter reduced abrupt spikes present in the original wave height signal. Also, there was little delay between the signals. However, as the wave frequency rises, so does the delay, and the signal tracking becomes less efficient.

After the qualitative analysis, it is necessary to obtain numerical evaluations of the improvement accomplished with the use of Kalman Filter. To do so, the method proposed by Schäffer (2001), was utilized to estimate the absorption efficiency. The author defines the re-reflection coefficient (Eq. 23) as the amount of waves that are not absorbed by the flaps and return to the model in the tank. Theoretically, this coefficient would be zero in a case of perfect absorption. In the real basin, it is desired this coefficient to be as low as possible.

$$RR = \frac{\tilde{A}_i}{\tilde{A}_r} \quad (23)$$

where \tilde{A}_i is the amplitude of waves not completely absorbed by the flaps and \tilde{A}_r is the amplitude of waves that strike the flaps.

For regular waves, again, two analyses were held. In each, waves with 4 different frequencies (0.75, 1.00, 1.25 and 1.50 Hz) were generated, one at a time. The first analysis was made with the flap mapping enabled (i.e., only good sensors were active and some flaps used adjacent flap sensors as reference). In the second analysis, the mapping was removed and all the flaps were controlled independently (each flap using its own sensor as reference). The re-reflection coefficient was calculated for both cases and the result is shown in Fig. 10, below.

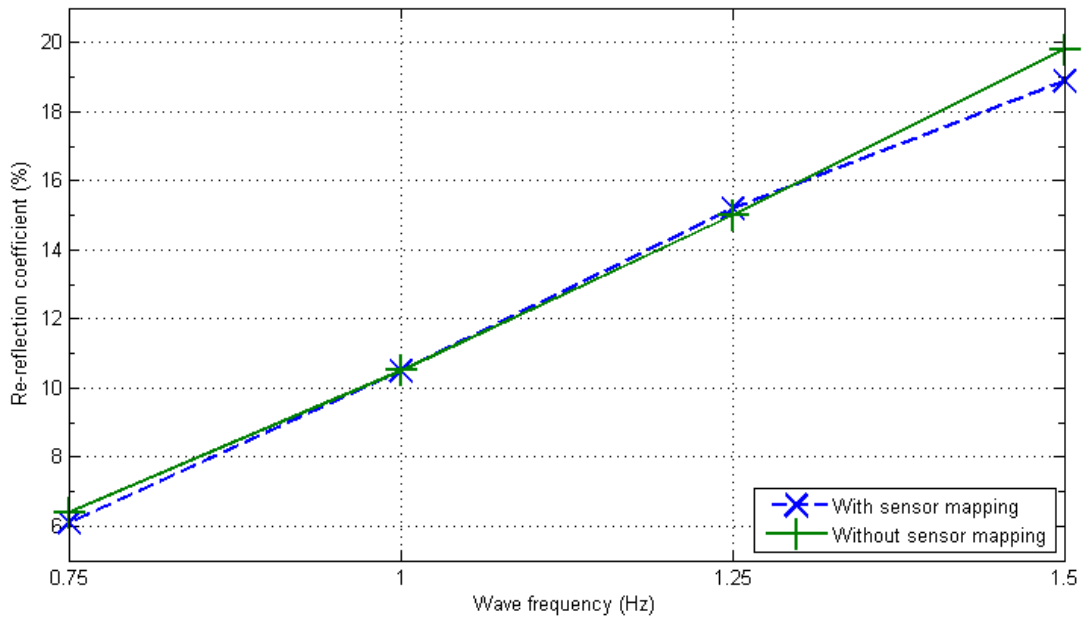


Figure 10. Re-reflection coefficient versus regular wave frequency, with Kalman Filter enabled

By the plot, little difference can be noticed between both analyses, thus indicating that the Kalman Filter had good performance even without the sensor mapping, i.e., even with the use of bad quality original wave height signals. Therefore, it is possible to disable the mapping, and better absorption of waves with different directions than the perpendicular to the flaps can be achieved.

For irregular waves, four sets of trials were made: the first using the Butterworth filter and other three using the Kalman Filter, each with different combination of Q and R Kalman parameters. Then, the curves of re-reflection coefficient versus wave frequency were calculated. The curves plot can be seen in Fig. 11.

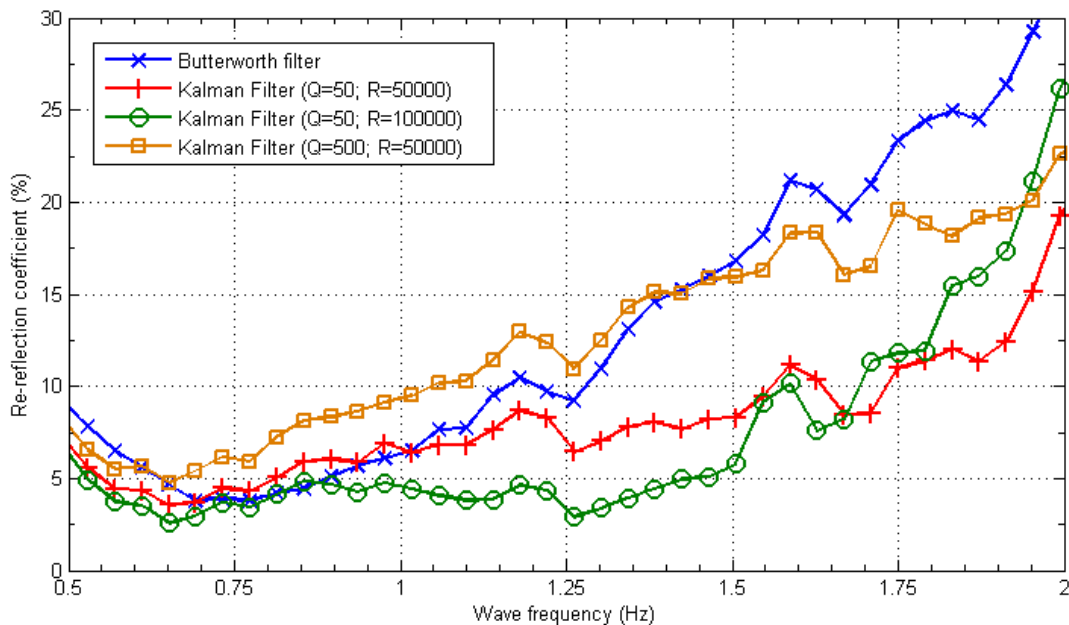


Figure 11. Re-reflection coefficient versus wave frequency for irregular waves

This is an interesting result. The Kalman Filter shows some improvement in the wave absorption for determined frequency intervals, but not for the entire spectrum in which the basin operates. In Fig. 11 it is clear to visualize the intervals in which the Kalman Filter surpasses the low pass filter (the lower the curve is, the best the absorption is).

5. CONCLUSION

The utilization of the Kalman Filter proved to be an interesting option to solve the problem of noise and distortion present in the wave height signals. However, there are still challenges to overcome regarding to the algorithm processing time inside CH-TPN control loop.

The use of control computer's graphics card to perform some calculations helped to decrease the Filter's processing time, but only enough to work with a full wall of the tank (39 flaps).

Even with the constraints of processing time given, the results obtained using the Kalman Filter indicated satisfactory noise attenuation and delay reduction, which considerably contributes to the improvement, as demonstrated, of absorption rates, compared with the Butterworth filter. The implementation of the Kalman Filter stands out even by allowing the removal of the sensor mapping, enabling the absorption of waves in all directions.

Finally, bearing in mind that the processing time problem can be overcome, for example, with the advance of technology or investment in a more powerful machine to run the control algorithm, the Kalman Filter is presented as a relevant solution to improve absorption rates of the CH-TPN to levels compatible with its design

6. ACKNOWLEDGEMENTS

The authors acknowledge Petrobras for the financial support and for the motivation of this work. The fourth author acknowledges the São Paulo State Research Foundation (FAPESP Proc. No. 2008/06428-4). The last author acknowledges the National Council for Scientific and Technological Development (CNPq) for the research grant (301686/2007-6).

7. REFERENCES

- Araujo, A. A. M., Lima, R. L., Tannuri, E. A., 2010, "Aplicação de Filtro de Kalman ao sensoriamento de nível baseado em sensores ultrassônicos do CH-TPN", Final Project presented to Escola Politécnica da Universidade de São Paulo (EPUSP).
- Carneiro, M. L., Mello, P. C., Labate, F. D., Araujo, A. A. M., Simos, A. N., Tannuri, E. A., 2009, "USP Wave Basin: Active wave absorption and generation algorithms", Proceedings of the 4th International Workshop on Applied Offshore Hydrodynamics, Rio de Janeiro, Brazil.
- Fossen, T. I., 1994, "Guidance and Control of Ocean Vehicles", Wiley, 494 p.
- Grewal, M. S., Andrews, A. P., 2008, "Kalman Filtering: Theory and Practice Using MATLAB", 3rd Edition, Wiley, 592 p.
- Kalman, R. E., 1960, "A New Approach to Linear Filtering and Prediction Problems", Transactions of the ASME – Journal of Basic Engineering, Vol. 82, Series D, pp. 35–45.
- Mello, P. C., Carneiro, M.L., Tannuri, E. A., Nishimoto, K., "USP Active Absorption Wave Basin: From Conception to Commissioning", Proceedings of the ASME 29th International Conference on Ocean, Offshore and Arctic Engineering OMAE 2010, 2010, Shanghai.
- Schäffer, H. A., 2001, "Active Wave Absorption in Flumes and 3D Basin". Proceedings of Ocean Wave Measurement and Analysis, pp. 1200–1208, 2001.
- TPN. "Tanque de Provas Numérico". 12 Oct. 2010. <<http://tpn.usp.br>>.

8. RESPONSIBILITY NOTICE

The authors are the only responsible for the printed material included in this paper.